Study of the Influence of Radionuclide Biokinetic Distribution in Human Body on the Efficiency Response of Lung Counters

LIU Liye [1, 2, *], CAO Qinjian [1], ZHAO Yuan [1], WEI Xiaofeng [1], XIAO Yunshi [1], XIONG Wanchun [1], PAN Hongjuan [1], CHEN Baowei [1], LI Junli [2]

[1] China Institute for Radiation Protection, Taiyuan, 030006, China
[2] Department of Engineering Physics, Tsinghua University, Beijing, 100084, China

Abstract

Reliable efficiency calibration of measuring systems is one of the most crucial tasks in *in-vivo* monitoring. The traditional calibration method is based on physical phantoms, such as the Livermore torso phantom for efficiency calibration purpose for lung counters. However, besides the shape of physical phantom does not represent realistic human anatomy faithfully, it is difficult for physical phantoms to simulate the non-uniformly source distribution in human body. Numerical calibration technique being the state-of-art provides a tool to investigate the above issue. In this paper, numerical calibration method is developed based on the Chinese Reference Adult Male (CRAM) voxel model, MCNP code, and the radionuclide biokinetics distribution data predicted by ICRP biokinetic model. Then, it is applied to study the influence of radionuclide biokinetic distribution in body on the detection efficiency of lung counter configured with four HPGe detectors. The preliminary results reveal that the radionuclide activity could be overestimated up to 50% (AMAD=1μm), 150% (AMAD=5μm) for ^{241}Am in the early period (<3d) after acute inhalation; and a relative flat response exists for the period from 3d to 100d, in which the overestimation are 10%-40% for 1μm, and 20%-60% for 5μm respectively; however, the overestimation would become worse along with the time extended, e.g., 160% and 230% for 1μm and 5μm respectively at 300d.

Keywords: Monte Carlo; efficiency calibration; in-vivo monitoring; voxel phantom; biokinetic

***Corresponding author:** liuliye@cirp.org.cn

1. Introductions

Physical phantoms, such as the Livermore torso phantom, are commonly used to calibrate the detection efficiency of lung counters, which usually has a uniformly activity distribution in lungs and ignores the photons contribution from the other interferential organs. However, the real activity distribution in human body is neither only located in lungs, nor as a uniformly distribution within body due to the biokinetic metabolism. Moreover, the activity distribution in the body varies with time following the intake as predicted by the biokinetic models. Thus, the physical phantom calibration process with the uniform and static source distribution assumption may lead to a biased measurement. Numerical calibration technique, also called virtual calibration method, has been developed by using human voxel phantoms and Monte Carlo simulation codes in recent years. It gives a more realistic anatomical representation of human body than the physical phantoms, and provides a powerful capability to simulate the biokinetic activity distribution in the human body.

By taking the advantage of virtual calibration technique, it is the intension of this paper to investigate the influence of biokinetic distribution of ^{241}Am within body on the detection efficiency of the lung counter, which is configured with four high-purity

germanium (HPGe) detectors.

2. Materials and Methods

2.1 Numerical calibration technique

Numerical calibration technique used in this paper has been developed based on human voxel phantoms and MCNP code, and validated by using physical phantom experiments in the previous studies [1,2,3]. A brief introduction will be given here.

Firstly, as shown in figure 1, the geometry model of HPGe detectors should be described properly in MCNP input file. The detectors' parameters, i.e., the diameter, length and dead-layer of Ge crystal, was adjusted carefully according to the measured efficiency by using point sources experiments, which could achieve a good agreement within 5% for photons with energy from 17.5keV—1332keV. Then, the virtual calibration process coupled with voxel phantom was validated by using the physical phantom with ^{241}Am lung sources. The CIRP-RPT-1 physical phantom was used for this purpose, which was developed in our institute for representing Chinese adult male anatomy. It has been confirmed that the relative deviations of detection efficiency between voxel phantom calculation and the physical phantom measurement are within ±15%, ±30% for 59.5keV and 17.5 keV photons, respectively.

Fig.1 the detector model, CIRP-RPT-1 phantom, the experimental arrangement, the virtual calibration (from left to right)

2.2 CRAM phantom and biokinetic model

The CRAM voxel phantom representing Chinese Reference Adult Male was used in this study [4]. There are more than 80 tissues and organs in CRAM, and the mass of individual organs has been adjusted to the Chinese reference data. As well-known, there are also many regions, called compartments, defined in the ICRP biokinetic model, such as ET1 (anterior nasal passage of extrathoracic airway), ET2 (posterior nasal and oral passage), BB (trachea and bronchi), bb (bronchiolar), and AI (the gas exchange region) in respiratory tract model. In order to simulate the activity biokinetic distribution in human voxel phantom, it is need to couple the CRAM phantom to the biokinetic model accordingly. Extra efforts have been made to sub-segment the respiratory tract into ET1, ET2, BB and lungs (AI+bb) in CRAM phantom as shown in figure 2. Meanwhile, the sub-segmentations were also made to the alimentary tract to separate the organs' wall from their content, such as stomach, small intestine (SI), upper large intestine (ULI), lower large intestine (LLI), etc., as shown in table 1.

The DCAL software was used to calculate the ^{241}Am biokinetic distribution in human body for different blood absorption types and particle sizes (AMAD), after an acute inhalation intake [5]. Generally, there are two methods for incorporating the activity distribution data into CRAM voxel model to calculate the detection efficiency. One is to

sample the source position and its activity in body synchronously during the Monte Carlo simulation, but with a time consuming process. Another more convenient way, used in this study, is to calculate the organ-specific detection efficiency for each organ in advance, and then to be multiplied by their corresponding activity content to obtain the total detection efficiency.

The CRAM phantom and the position of four HPGe detectors, the activity in organs as the function of time calculated by DCAL, and the organ-specific detection efficiency are shown in figure 3(a), 3(b), and 3(c) respectively. The changing of activity along with time in CRAM phantom is shown graphically in figure 4.

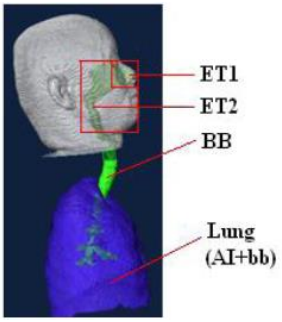

Fig. 2 Segmentation of respiratory tract in CRAM voxel phantom

Table 1 The corresponding organs in CRAM and biokinetic model

CRAM	Biokinetic model	CRAM	Biokinetic model
ET1	ET1, LN-ET	Stomach-Cont.	St-Cont.
ET2	ET2	Small Intestine -Cont	SI-Cont.
BB	BB	ULI-Cont.	ULI-Cont.
Lungs(left/right)	AI, bb, LN-lung	LLI –Cont.	LLI-Cont.
Liver	Liver	Kidneys (left/right)	Kidneys
Cortical bone	CBone-S/V	UB-Content	UB-Cont.
Trabecular bone	TBone-S/V, RBM	Others	Body, Blood, LN, etc.

Remarks: LN—lymph nodes, RBM—Red Bone Marrow, S/V—Surface/Volume, UB—Urinary bladder

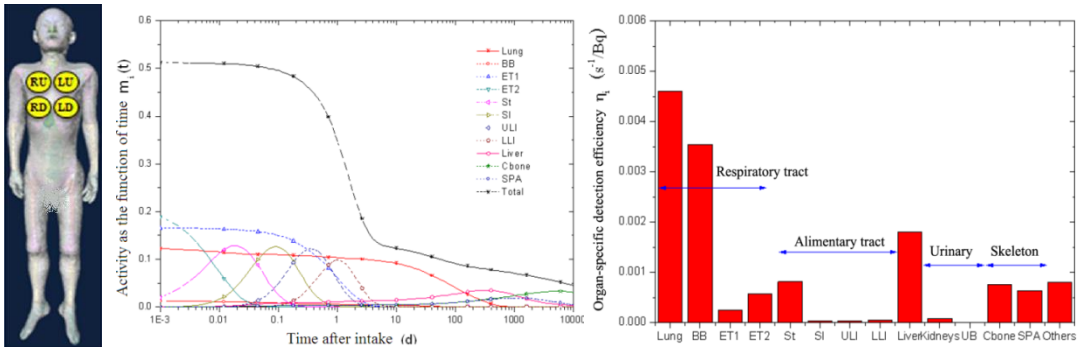

(a) (b) (c)

Fig.3 CRAM phantom and four HPGe detectors (a) , ^{241}Am biokinetic distribution data (b), and the pre-calculated organ-specific detection efficiency (c).

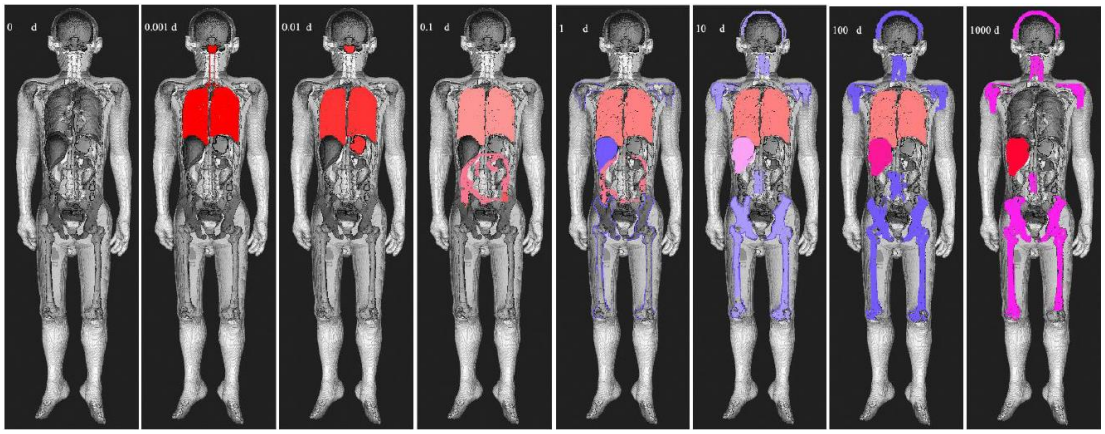

Fig.4 Visualization of activity distribution in CRAM phantom as the function of time

2.3 Calculation of the influence of biokinetics activity distribution

The usual formula to calculate the intake by using physical phantom calibration method can be described as the follows:

$$I_{\mathrm{hom}} = \frac{n_o(t)}{\eta_{Lung} \cdot m_{Lung}(t)} \qquad (1)$$

Where，I_{hom} is the intake calculated by using the traditional calibration factors, which is obtained by assuming that the activity is only uniformly located in lungs; $n_o(t)$ is the total net count rate of the detectors (counts/s), $m_{Lung}(t)$ is the activity in lungs as the function of time, η_{Lung} is peak detection efficiency of lung source for 59.5 keV photons (counts/s/Bq).

When considering the time-dependent biokinetic activity distribution in the human body and its influence on the detection efficiency, the intake should be calculated as formula (2):

$$I_{\mathrm{Bio}} = \frac{n_o(t)}{\sum \eta_i \cdot m_i(t)} \qquad (2)$$

Where, $n_o(t)$ is the total net count rate of the four detectors (counts/s), $m_i(t)$ is the activity in organ i as the function of time, η_i is the organ-specific peak detection efficiency for 59.5 keV photons (counts/s/Bq).

The difference between I_{hom} and I_{Bio} can be calculated as formula (3), which indicates the errors of traditional calibration method for lung counting measurement.

$$\mathrm{err} = \frac{I_{\mathrm{hom}} - I_{Bio}}{I_{\mathrm{Bio}}} = \frac{\sum \eta_i \cdot m_i(t)}{\eta_{Lung} \cdot m_{Lung}(t)} - 1 \qquad (3)$$

3. Results

The errors of intake measurement by traditional calibration method are shown in figure 5, for ^{241}Am aerosol acute inhalation with different absorption types (M, S) and particle sizes. The preliminary results reveal that:

(1) For M absorption type, the intake activity can be significantly overestimated up to 50% for AMAD=1μm, 150% for AMAD=5μm, and even 2000% for AMAD=100μm in

the early period following intake (t<3d). And the overestimation becomes worse along with the bigger particle size. There is a relative flat response region for the period from 3d to 100d, in which the overestimations are 10%-40% for 1μm and 20%-60% for 5μm respectively. These results quantitatively agrees with those reported in the study by Lamart *et al.*, in which it is reported that the overestimations are 30% and 40% for AMAD=1μm, 5μm respectively at the time of 100d after intake [6]. However, the overestimation would become worse along with the time extended, e.g., 160% and 230% for 1μm and 5μm respectively at 300d.

(2) For S absorption type, similar to that of M-type, the intake activity can be overestimated up to 40% for AMAD=1μm, 140% for AMAD=5μm in the early period following intake (t<3d). There is also a good flat response region for the period from 3d to 1000d, in which the overestimations are less than 5% for all particle sizes. However, the overestimation would become worse along with the time extended, e.g., 10% (2000 d), 20% (3000 d), 30% (4000 d)、40% (5000 d) and 100% (10000 d).

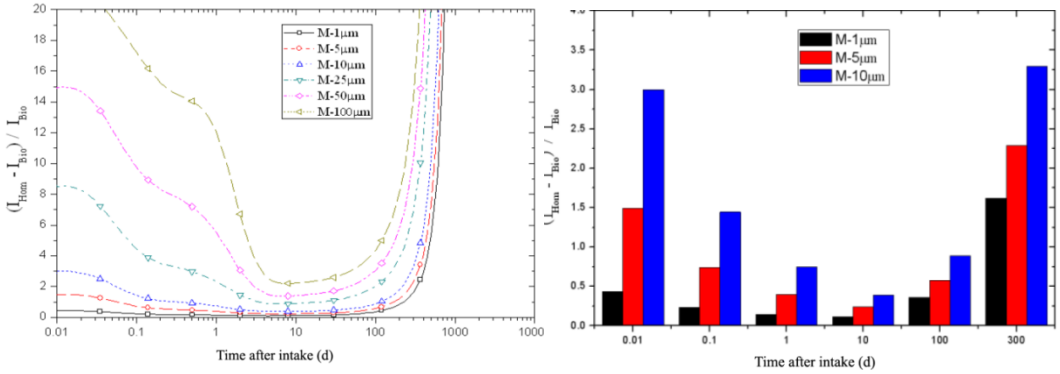

Fig. 5 (a) Errors as the function of time for ^{241}Am with the absorption type of M

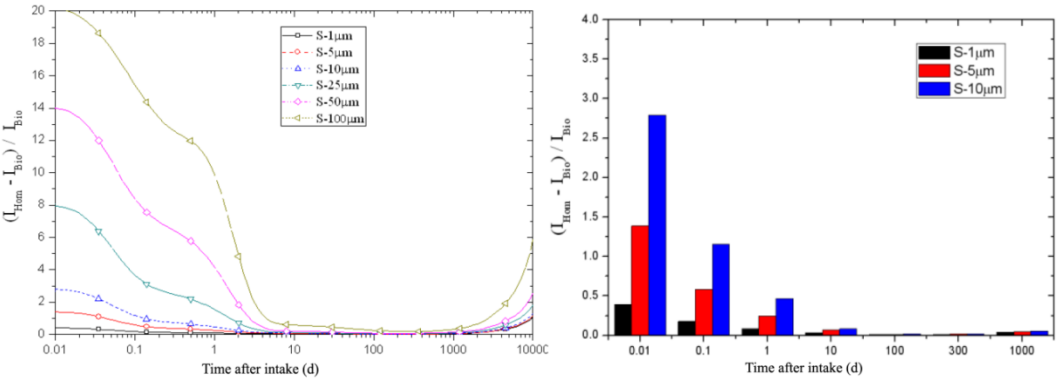

Fig. 5 (b) Errors as the function of time for ^{241}Am with the absorption type of S

4. Discussions

By using the biokinetic distribution data and the organ-specific detection efficiency as shown in figure 3(b) and 3(c), the preliminary results in the above section can be explained as follows: (1) It is known that the particle size (i.e, AMAD) has a great influence on the radionuclide deposition pattern in body in the early period after acute inhalation. There is more activity deposited in the ET1, ET2 regions along with the larger particle size, some of which are then entered into stomach. So the overestimation of intake is worse for larger particle size in the early period. However, the activity in ET and stomach regions will be excreted out beyond 3 days, so it is reasonable that there is a flat

response period from 3d to 100d (for M-type) and to 1000d (for S-type). (2) The absorption type has a great influence on the biokinetic distribution for long-term period. It can be seen that the activity with M-absorption type will be accumulated in the liver and skeleton as the time passed, so the detection efficiency response becomes worse for the time beyond 100d. However, due to it is difficult for S-type aerosol to be absorbed by blood, i.e., most of the activity retains in lungs, thus, the estimation of intake for S-type could be considerable better than M-absorption type.

References

[1] Qinjian CAO, Binquan ZHANG and Hongjuan PAN, Research on the virtual calibration technique for the lung counting system in internal exposure, The Third Asian and Oceanic Congress on Radiation Protection (AOCRP-3) ,May 24-28, 2010, Tokyo, Japan.

[2] LIU Liye, D. Franck, L.D. Carlan, LI Junli, Application of Monte Carlo calculation and OEDIPE software for virtual calibration of an in vivo counting system, Radiation Protection Dosimetry,127(1-4)(2007):282-286.

[3] LIU Liye, D. Franck, L.D. Carlan, MA Jizeng, Voxel phantom based on the CT images of Livermore torso phantom and its application for virtual calibration of a real in-vivo lung counting system, Radiation Protection, 27(5) (2007): 264-271.

[4] LIU Liye, ZENG Zhi, LI Junli, QIU Rui , ZHANG Binquan, MA Jizeng, REN Li, LI Wenqian, and BI Lei, Organ dose conversion coefficients on an ICRP-based Chinese adult male voxel model from idealized external photons exposures, Physics in Medicine and Biology 54(2009): 6645-6673.

[5] Eckerman KF, Leggett RW, Cristy M, et al , User‘s Guide to the DCAL System, ORNL/TM-2001/190, 2006.

[6] Lamart S, Blanchardon E, Molokanov A, et al, Study of the influence of radionuclide biokinetics on the efficiency of in vivo counting using Monte Carlo simulation. Health Physics, 2009, 96(5): 558-567.